

COMPARATIVE BIOLOGICAL ACTIVITY OF PHYTOMEDIATED ZINC, COPPER, AND HYBRID NANOPARTICLES

HALEEMA BIBI

MS Student, Institute of Biotechnology and Microbiology (IBM), Bacha Khan University, Charsadda, Pakistan. Email: haleemagull32@gmail.com

Dr. FARHAD ALI

Assistant Professor, Institute of Biotechnology & Microbiology, Bacha Khan University, Charsadda, Pakistan. Corresponding Author Email: drfarhad@bkuc.edu.pk, Orcid Id: 0000-0002-8649-558X

TAHIR SALAM

MS Student, Institute of Biotechnology and Microbiology (IBM), Bacha Khan University, Charsadda, Pakistan. Email: tahirsalam.biotech@bkuc.edu.pk, Orcid Id: 0000-0003-4627-5758

Dr. AJMAL KHAN

Assistant Professor, Institute of Biotechnology & Microbiology, Bacha Khan University, Charsadda, Pakistan. Email: ajmalkhan@bkuc.edu.pk

Dr. SAEED AHMAD

Assistant Professor, Institute of Biotechnology & Microbiology, Bacha Khan University, Charsadda, Pakistan. Email: sangolians@gmail.com

IFTIKHAR AHMAD

MS Student, Institute of Biotechnology and Microbiology (IBM), Bacha Khan University, Charsadda, Pakistan. Email: hamdardbuneri7@gmail.com

Abstract

Green synthesis of metal nanoparticles (NPs) has attracted considerable attention because of its cheaper protocols and is more environmentally friendly than standard synthetic methods. In the present study, we report the green synthesis of zinc oxide nanoparticles (ZnO NPs) and copper oxide nanoparticles (CuO NPs) by using Caralluma tuberculata stem extract. ZnO NPs and CuO NPs were characterized by using UV-Visible Spectroscopy, Fourier Transform Infrared Spectroscopy (FTIR), Scanning Electron Microscopy (SEM), and Energy Dispersive X-ray Spectroscopy (EDX). UV-Visible absorption data of ZnO NPs and CuO NPs showed the characteristic absorption peak at 380 nm and 460nm. FTIR analysis confirmed the capping of nanoparticles by phytochemicals present in Caralluma tuberculata, which showed absorption bands in the range of 3500-3000 cm^{-1} , 1700-1600 cm^{-1} , 1000 cm^{-1} , and below 900 cm^{-1} . SEM revealed the morphological features of the synthesized ZnO NPs and CuO NPs with an average size of 40 nm and 60 nm, respectively. EDX spectroscopy of ZnO NPs shows two peaks of zinc at 1 keV and 8.5 keV, and a single peak for oxygen atoms at 0.5 keV. For CuO NPs two strong peaks of copper at 1keV and 8 keV, and a single peak for oxygen atom at 0.5 keV was observed, affirming the purity and successful synthesis of crystalline metal oxide nanoparticles. Synthesized ZnO NPs showed tremendous antibacterial activity against S. aureus and Acetobacter strains. CuO NPS showed significant activity against S. aureus, while moderate activity against Acetobacter. A Hybrid of ZnO NPs and CuO NPs showed considerable activity against both tested bacteria. The acetone extract was equally effective against both strains, while aqueous and mixed extract was more effective against S. Aureus than Acetobacter. Furthermore, the photocatalytic activity of ZnO NPs and CuO NPs was examined by degradation of xylene dye and congo red dye under

UV light. ZnO NPs degraded 60% of xylene dye, while CuO NPs degraded 90% of Congo red dye in 30 minutes.

Keywords *Caralluma tuberculata*, ZnO NPs, CuO NPs, Phytochemicals, UV, FTIR, SEM, EDX, Antibacterial activity, Photocatalytic activity.

CHAPTER 1

INTRODUCTION

The most common definition of nanotechnology is manipulation, observation, and measurement at a scale below 100 nanometers [1]. Nanotechnology can simply be defined as the technology at one-billionth of a meter scale. It is the ability to work at the atomic, molecular, and super-molecular levels to create and employ materials, structures, devices, and systems with basically new properties [2]. Nanotechnology is emerging as a new field of research dealing with the synthesis of nanoparticles and nanomaterials for their applications in various areas such as electrochemistry, catalysis, sensors, biomedicines, pharmaceuticals, health care, cosmetics, food technology, textile industry, mechanics, optics, electronics, space industry, energy science, and optical devices, etc. (3-9). Nanotechnology is a broad area and has also shed a ray of light on the field of biotechnology and medicine [10]. The nanoparticles have been synthesized using physical, chemical, and biological methods. Where the physical techniques have a low yield, while chemical processes use various toxic chemical agents to reduce metallic ions to nanoparticles, which is often harmful to the biological systems. The chemical method also generates hazardous by-products [11]. Synthesis of nanoparticles by biological methods, using microorganisms, enzymes, and plant or plant extract, has been suggested as a possible eco-friendly alternative to chemical and physical processes [12]. The phytochemicals responsible for the synthesis of nanoparticles are terpenoids, flavonoids, carbohydrates, saponins, alkaloids, and proteins. Greener synthesis of nanoparticles provides advancement over other methods as it is simple, cost-effective, and relatively reproducible and often results in more stable materials [13]. Metallic NPs used in therapy and diagnosis must be nontoxic, biocompatible, and stable. Furthermore, they must selectively address the desired target [14]. Zinc oxide (ZnO) nanoparticles exhibit antibacterial, anti-corrosive, antifungal, and UV filtering properties.

CHAPTER 2

MATERIAL AND METHODS

Plant material:

Caralluma tuberculata stem was used to prepare extract for the synthesis of zinc and copper nanoparticles.

Preparation of *Caralluma tuberculata* stem Extract:

A fresh young plant of *Caralluma tuberculata* was obtained from the local market, and the stem was separated from the collected plant. 100g of *Caralluma tuberculata* stem was washed several times with tap water, 3 times with ethanol, and 3 times with distilled water to remove dust particles and other impurities, and 100g of the stem were kept in a water bath at 90°C for 30 mins in 400ml of distilled water. The stem was crushed with the help of a grinder, and 100ml acetone was added and the mixture was stored for 24 hours at room temperature. The extract was centrifuged at 6500rpm for 15 minutes, the pellet was discarded, and the supernatant was filtrated using Whatman No.1 filter paper. The filtered extract was stored at room temperature for further studies.

Synthesis of zinc nanoparticles:

0.01M aqueous solution of zinc sulfate heptahydrate was prepared and used for the synthesis of zinc nanoparticles. Briefly, 100 ml of *Caralluma tuberculata* extract was added into 100 ml of an aqueous solution of 0.01M zinc sulfate heptahydrate. An 8ml aqueous solution of 0.01M NaOH was added under vigorous stirring at 90°C for 4 hours on a hot plate. The synthesis of nanoparticles was confirmed by the change in color of the solution from colorless to green, as shown in Fig 2.1. The solution was filtered using Whatman No. 1 filter paper. The zinc nanoparticles on the surface of Whatman No. 1 filter paper were then put in centrifuge tubes and washed once with ethanol and then two times with distilled water at 6500 rpm for 15 minutes. After washing, the nanoparticles were dried in an oven and stored in Eppendorf tubes for further studies.

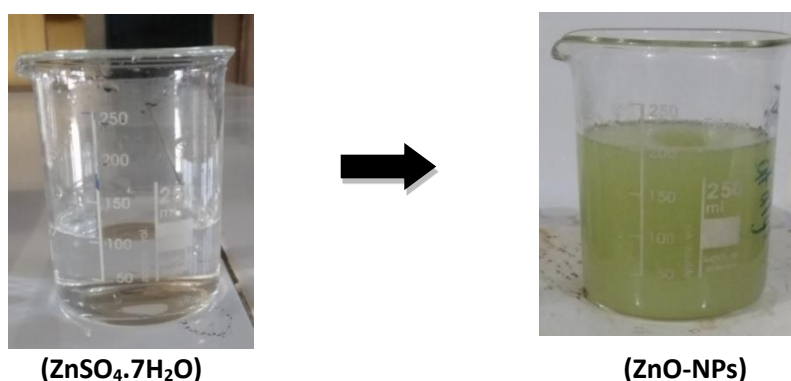


Fig 2.1: Pictures show a change in the color of the solution from colorless to green.

Synthesis of copper nanoparticles:

0.01m aqueous solution of copper sulfate pentahydrate was prepared and used for the synthesis of copper nanoparticles. Briefly, 100 ml of *Caralluma tuberculata* stem extract was added into 100 ml of an aqueous solution of 0.01m copper sulfate pentahydrate under vigorous stirring at 90°C for 4 hours on a hot plate. The synthesis of particles was confirmed by the change in solution color from sky blue to sea green, as shown in Fig 2.2. The solution was dried on a hotplate, and prepared particles were obtained and washed once with ethanol and twice with distilled water in a centrifuge at 6500 rpm for 15 mints. After washing, the nanoparticles were dried in an oven and stored in Eppendorf tubes for further studies.

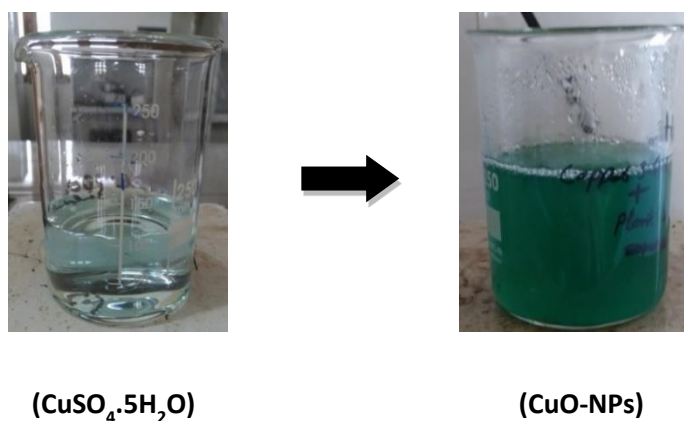


Fig 2.2: Pictures show a change in color of the solution from sky blue to sea green

Photocatalytic Degradation of Xylene Dye by Zn-NPs:

Xylene dye was subjected to photo-degradation using the synthesized ZnO NPs under UV light to investigate its photocatalytic activity. A 100ppm solution of xylene dye was prepared by dissolving 0.005g of xylene dye in 500 ml distilled water. From this stock solution, take 10ml solution, add 0.002gm of ZnO-NPs, and place the resultant solution under UV light to observe photocatalytic degradation. The absorption spectra were recorded for the clear dye solutions at 610 nm for xylene dye using a UV-Vis spectrophotometer to determine the remaining dye concentration. ZnO nanoparticle suspension with xylene dye was exposed at different time intervals (5, 10, 15, 20, 25, and 30 minutes). And the concentration of xylene dye in the resultant solution was monitored in the wavelength range of 200-800 nm in a UV-visible spectrophotometer.

Photocatalytic Degradation of Congo red Dye by Cu-NPs:

Photocatalytic degradation activity of the CuO nanoparticles was estimated by the degradation of Congo red dye under UV light. For this assay, make a 100ppm solution of Congo red dye by dissolving 0.005g of Congo red dye in 500ml distilled water. From this stock solution, take 10ml solution and add 0.002g of CuO NPs, and place under UV light. The absorption spectra were recorded for the clear dye solution at 490 nm for Congo red dye using a UV-Vis spectrophotometer to determine the remaining dye concentration. CuO nanoparticle suspension with Congo red dye was exposed at different time intervals (5, 10, 15, 20, 25, and 30 minutes). The concentration of Congo red dye in the resultant solution was monitored in the wavelength range of 200-800 nm in a UV-visible spectrophotometer.

U-Vis Spectrophotometer:

The reduction of zinc and copper ions was monitored by measuring optical density through UV-Vis spectroscopy of the reaction medium after diluting small aliquots of the reaction mixture with Milli-Q water and transferring to the cuvette and analyzed using a UV-Vis spectrometer.

FTIR analysis:

FTIR was used to identify the possible functional group involved in the reduction of zinc and copper and the capping of reduced zinc and copper nanoparticles. FTIR spectrum was recorded using Shimadzu, Japan, infrared double beam spectrometer.

SEM analysis:

The surface morphology of synthesized ZnO and CuO NPs was studied by observing the images captured under SEM. SEM slide was prepared by making a smear of solution on a slide. Then the slide was set for SEM analysis after coating the slide with platinum, and the SEM image was taken.

EDX analysis:

An energy-dispersive X-ray technique was employed to determine the composition of the synthesized CuO and ZnO nanoparticles. Energy-dispersive X-ray spectroscopy (EDX) supplied purity data of the synthesized NPs, and elemental mapping provided the distribution of the elements.

CHAPTER 3

RESULTS

CHARACTERIZATION

UV- analysis

UV-visible spectra of ZnO Nanoparticle:

The biologically reduced zinc sulfate heptahydrate precursor salt ($\text{ZnSO}_4 \cdot 7\text{H}_2\text{O}$) into zinc nanoparticles was characterized by a UV-visible spectrophotometer in an aqueous medium (i.e., deionized water). The quartz cuvette and deionized water were used as a standard, and the reading of the spectrophotometer was recorded at a scanning speed of 200-800nm. The λ - max was observed in the range of 380nm (Fig 3.1).

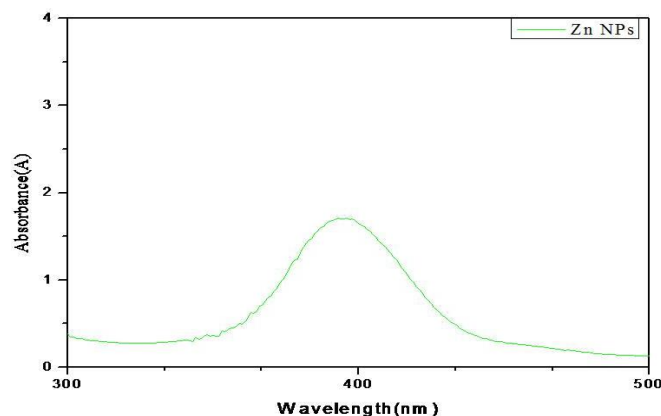


Figure 3.1: Uv-visible spectra of ZnO Nanoparticles

UV-visible spectra of CuO Nanoparticle:

The biologically reduced copper sulfate pentahydrate precursor salt ($\text{CuSO}_4 \cdot 5\text{H}_2\text{O}$) into copper nanoparticles was characterized by a UV-visible spectrophotometer in an aqueous medium (deionized water). The quartz cuvette and deionized water were used as a standard, and the reading of the spectrophotometer was recorded at a scanning speed of 200-800nm. The λ - max was observed in the range of 460nm (Fig 3.2).

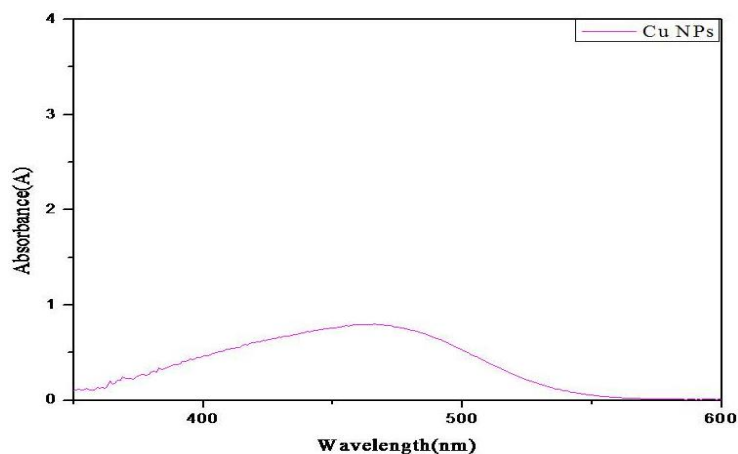


Figure 3.2: UV-visible spectra of CuO Nanoparticles

FT-IR analysis

FTIR ANALYSIS OF EXTRACT, ZnO NPs and CuO NPs:

Fig 3.3 shows the FT-IR spectra of aqueous, acetone, and mixed extract of *Caralluma tuberculata*. The Spectra show a broad peak in the range of $3500-3000\text{ cm}^{-1}$, possibly due to the -OH group in water, alcohol, and phenols. The spectra also show peaks in the region of $1600-1700\text{ cm}^{-1}$, which might be due to the stretching vibration of C=O in polyphenols and C=C stretch in aromatic ring and alkene. The peaks at 1000 cm^{-1} indicate the presence of C-N stretching of secondary aromatic amines and C-O stretching in amino acids. The acetone extraction shows peaks in the range of $3100-2900\text{ cm}^{-1}$ due to the stretching vibration of C-H. The acetone extraction sample also shows a peak at $1350-1250\text{ cm}^{-1}$, which might be due to the C-O-C glycosidic linkage in polysaccharides. The Spectrum of ZnO NPs shows peaks at about 1600 cm^{-1} , which might be due to the stretching vibration of C=O and C=C, and at 1000 cm^{-1} which might be C-N and C-O stretching. The spectrum also shows peaks between $800-550\text{ cm}^{-1}$ representing the metal nanoparticles indicating the successful synthesis of ZnO NPs (Fig 3.4). The Spectrum of CuO NPs shows a broad peak in the range of $3500-3000\text{ cm}^{-1}$, which might be due to the -OH group. The spectra also show peaks in the region of $1700-1600\text{ cm}^{-1}$, which might be due to the stretching vibration of C=O and C=O. The spectrum also shows a peak at 1000 cm^{-1} , which might be due to C-N and C-O stretching. The spectrum also presented peaks below 900 cm^{-1} , representing the metal nanoparticles indicating the successful synthesis of CuO nanoparticles (Fig 3.5).

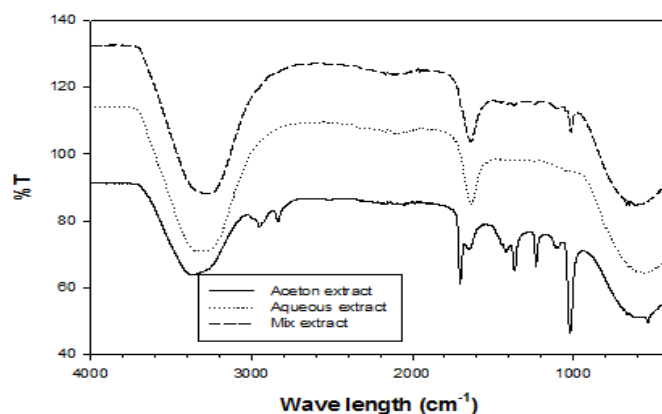


Fig 3.3: FTIR analysis of Extracts

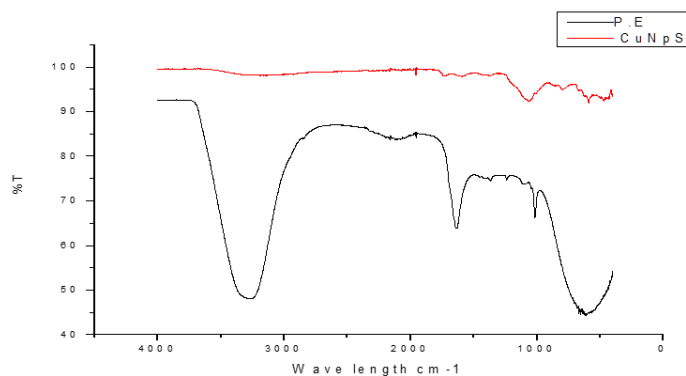


Fig 3.4: FTIR analysis of ZnO NPs

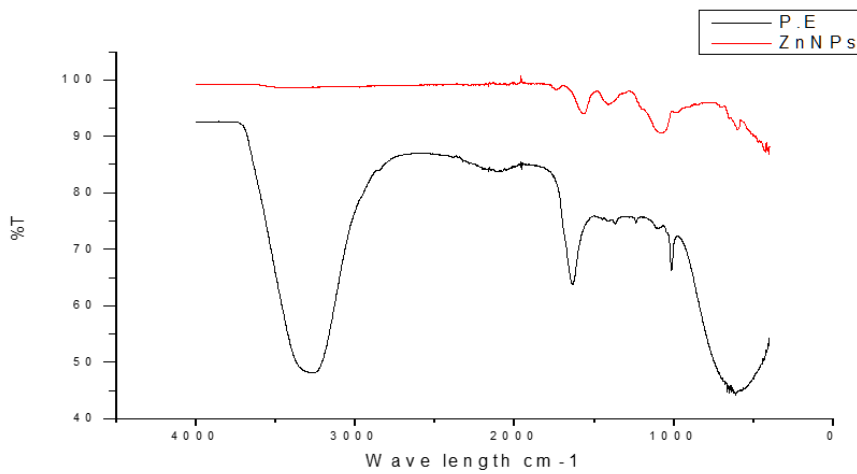


Fig 3.5: FTIR analysis of CuO NPs

SEM analysis

Analysis of ZnO Nanoparticles Using SEM:

It was concluded from the SEM images that synthesized ZnO NPs were spherical. The size of the ZnO NPs was also calculated using image j software as 40 nm, and the nanoparticles were dispersed, as shown in Fig 3.6.

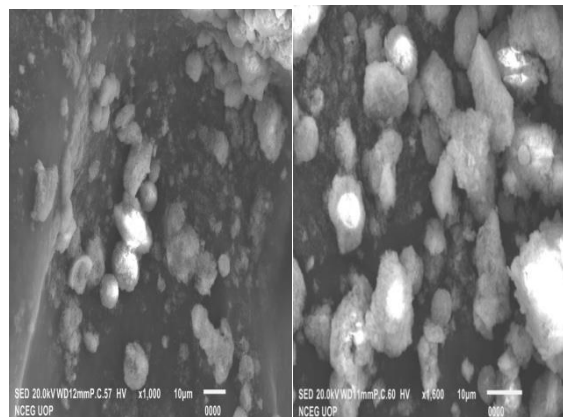


Fig 3.6: SEM images of prepared ZnO Nanoparticles.

Analysis of CuO Nanoparticles Using SEM:

The mean size of CuO NPs was calculated from SEM micrographs via ImageJ software and was found to be 60 nm. It was concluded from the SEM image that synthesized CuO nanoparticles were irregular in shape and were agglomerated (Fig 3.7).

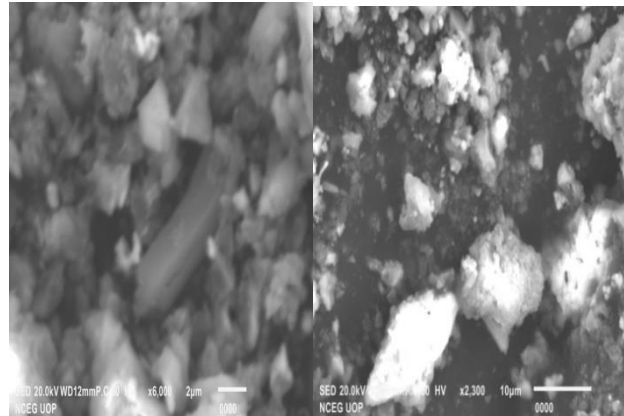


Fig 3.7: SEM images of prepared CuO Nanoparticles.

EDX analysis

EDX analysis of ZnO nanoparticles:

EDX studies were carried out to confirm the presence of ZnO nanoparticles and examine the prepared sample's chemical formation and composition (Fig 3.8). EDX spectroscopy of ZnO NPs shows two strong peaks of zinc at 1 keV and 8.5 keV, a single peak for oxygen atom at 0.5 keV, a peak for carbon atom at 0.2 keV, a peak for sulfur at 2.2 keV, with the weight percentage of zinc 34.69%, oxygen 39.30%, carbon 23.43%, sulfur 2.58%, affirmed the successful synthesis and purity of nanocrystalline Zn-NPs (Table 1). It is clear from Figure 8 that the EDX pattern confirmed the successful formation of ZnO nanoparticles with the stem extract of *Caralluma tuberculata*. The EDX peak positions were consistent with zinc oxide, and the sharp peaks of EDX indicated that the synthesized ZnO nanoparticles had a crystalline structure. The other two peaks observed in the EDX spectrum were due to impurities from C and S present in the substrate. The strong intensity and narrow width of ZnO diffraction peaks indicate that the resultant products were highly crystalline. Hence, we can conclude that green fuel played a profound role in controlling particle size.

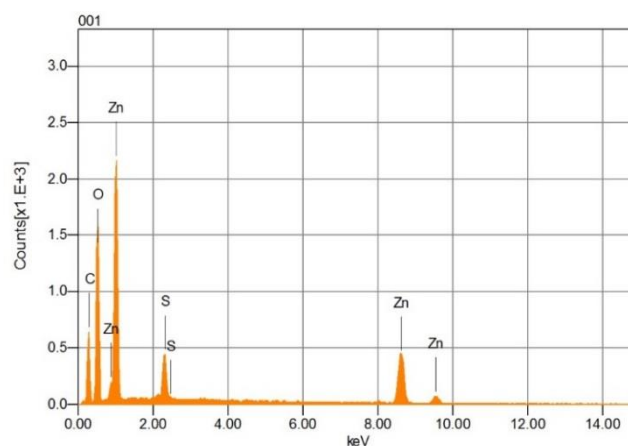


FIG 3.8: EDX analysis of ZnO NPs

Formula	mass%	Atom%	Sigma	Net	K ratio	Line
C	23.43	38.88	0.04	18901	0.0023840	K
O	39.30	48.95	0.11	60670	0.0349700	K
S	2.58	1.60	0.03	20452	0.0041997	K
Zn	34.69	10.58	0.20	55079	0.0642763	K
Total	100.00	100.00				

Table 3.1: EDX analysis of ZnO NPs

EDX analysis of CuO nanoparticles:

EDX studies were carried out to confirm the presence of CuO NPs and examine the prepared sample's chemical formation and composition (Fig 3.9). It confirms the presence of all constituent elements, i.e., copper (Cu), oxygen (O), carbon (C), sulfur (S), chlorine (Cl), potassium (k), and calcium (Ca), in the synthesized CuO nanoparticles. The EDX spectroscopy of CuO-NPs shows two strong peaks of copper at 1 keV, and 8 keV, a single peak for an oxygen atom at 0.5 keV, a peak for a carbon atom at 0.2 keV, a peak for sulfur at 2.5 keV, a small peak for chlorine at 2.8 keV, a small peak for potassium at 3.5 keV and a small peak for calcium at 3.8 keV with the weight percentage of 16.13% Copper, oxygen 35.42%, carbon 40.14%, sulfur 4.29%, chlorine 0.82%, potassium 1.39% and calcium 1.82% affirmed the successful synthesis and purity of nanocrystalline Cu-NPs. It is clear from Figure 9 that the EDX pattern confirmed the successful formation of CuO nanoparticles with the stem extract of *Caralluma tuberculata*. The EDX peak positions were consistent with copper oxide, and the sharp peaks of EDX indicated that the synthesized CuO NPs had a crystalline structure. The other peaks observed in the EDX spectrum were due to impurities from C, S, Cl, K, and Ca which were present in the substrate. The strong intensity and narrow width of CuO diffraction peaks indicate that the resultant products were highly crystalline.

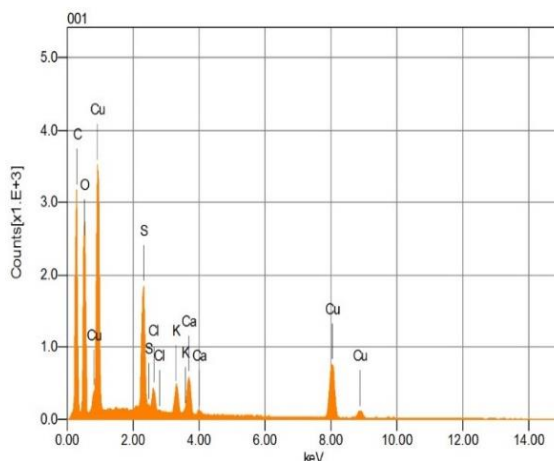


Fig 3.9: EDX analysis of CuO NPs

Formula	mass%	Atom%	Sigma	Net	K ratio	Line
C	40.14	55.26	0.03	81041	0.0102219	K
O	35.42	36.61	0.09	67822	0.0390922	K
S	4.29	2.21	0.02	75590	0.0155215	K
Cl	0.82	0.38	0.01	14899	0.0032559	K
K	1.39	0.59	0.02	21463	0.0057119	K
Ca	1.82	0.75	0.02	28533	0.0079826	K
Cu	16.13	4.20	0.08	59794	0.0585008	K
Total	100.00	100.00				

Table 3.2: EDX analysis of CuO NPs

Antibacterial Activity

Antibacterial activity of ZnO NPS and acetone extract:

ZnO NPs synthesized using *Caralluma tuberculata* extract were tested for antibacterial activity against *Staphylococcus aureus* and *Acetobacter*. The zone of inhibition for each tested bacteria was measured in millimeters (Table 3.3 and Fig 3.10). ZnO NPs were active against both the tested bacterial strains. The acetone extract was also found active against both strains.

S.NO	Bacteria strains	50µl	75µl	100µl	Acetone Extract
1.	<i>Staphylococcus aureus</i>	15mm	14mm	17mm	16mm
2.	<i>Acetobacter</i>	14.5mm	15.5mm	17mm	16mm

Table 3.3: Antibacterial activity of ZnO NPS and acetone extract

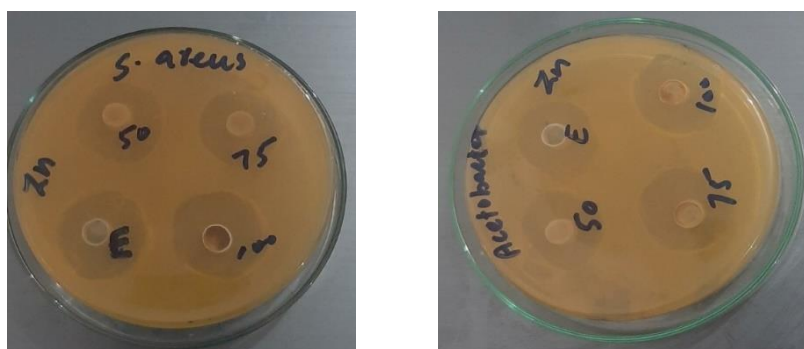


Fig 3.10: Antibacterial graph of ZnO NPs against *Staphylococcus aureus* and *Acetobacter*

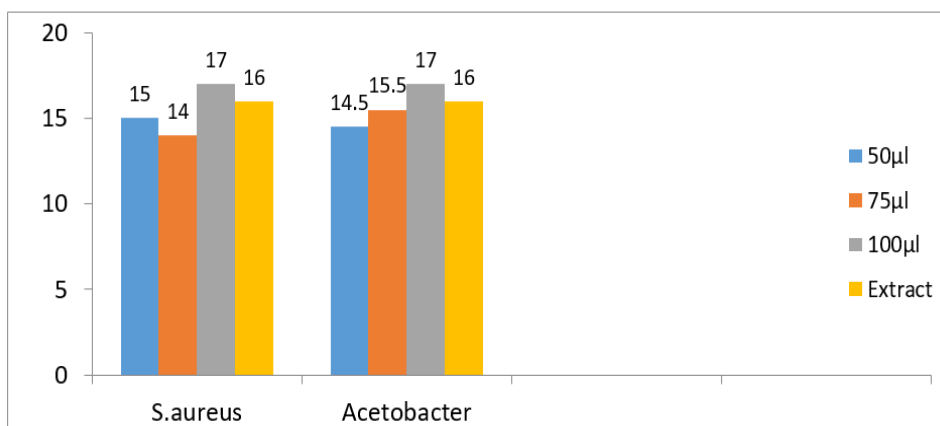


Fig 3.11: Pictures show the antibacterial activity of ZnO NPS against selected bacterial strains.

Antibacterial activity of CuO NPs and aqueous extract:

CuO NPs synthesized using *Caralluma tuberculata* extract were tested for antibacterial activity against *Staphylococcus aureus* and *Acetobacter*. The zone of inhibition for each tested bacteria was measured in millimeters as shown in table 3.4 and Fig 3.12. CuO Nps was active against both tested bacteria. CuO Nps showed significant activity against *Staphylococcus aureus* while the CuO NPs showed moderate activity against *Acetobacter*, and the aqueous extract was most effective against *Staphylococcus aureus* as compared to *Acetobacter*.

Table 3.4: Antibacterial activity of CuO NPS and aqueous extract

S.NO	Bacterial strains	50µl	75µl	100µl	Aqueous extract
1.	<i>Staphylococcus aureus</i>	18mm	19mm	19.5mm	16 mm
2.	<i>Acetobacter</i>	14.5mm	15.5mm	12.5mm	13mm

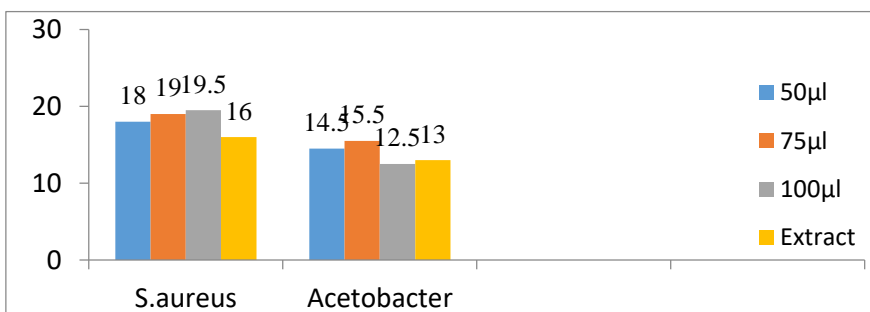


Fig: 3.12 Antibacterial graph of CuO NPs against staphylococcus aureus and Acetobacter



Fig 3.13: Pictures show the antibacterial activity of CuO NPS against selected bacterial strains

Antibacterial activity of ZnO NPs and CuO NPs hybrid and mix extract:

CuO NPs and ZnO NPs hybrid were tested for antibacterial activity against *Staphylococcus aureus* and *Acetobacter*. The zone of inhibition for each tested bacteria was measured in millimeters as shown in Table 3.5 and Fig 3.14. Hybrid NPs were active against both of the tested bacterium. Mix extract was most effective against *Staphylococcus aureus* as compared to *Acetobacter*.

S.NO	Bacteria strains	50µl	75µl	100µl	Mix-extract (acetone+aqueous)
1.	<i>Staphylococcus aureus</i>	15mm	13mm	16.5mm	16.5mm
2.	<i>Acetobacter</i>	10mm	13mm	15mm	14 mm

Table 3.5: Antibacterial activity of CuO and ZnO NPs hybrid and mix extract

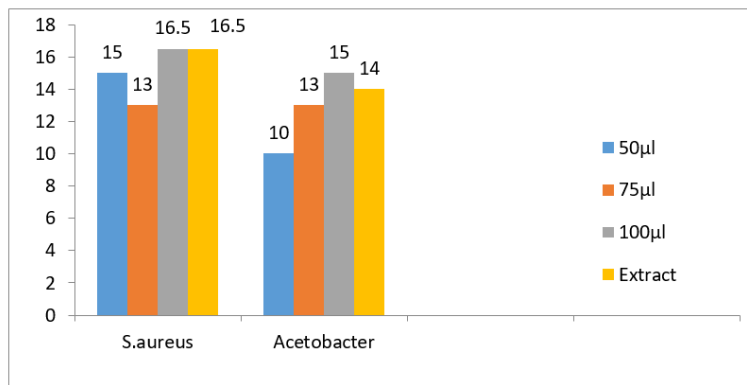


Fig 3.14: Antibacterial graph of ZnO NPs and CuO NPs hybrid against Staphylococcus aureus and Acetobacter



Fig 3.15: Pictures showed antibacterial activity of CuO and ZnO NPS hybrid against selected bacterial strains.

Photocatalytic degradation of xylene dye by ZnO NPs

The photocatalytic degradation of xylene dye under visible light was studied to check the removal of dye by measuring the decrease in absorbance of dye in the presence of the synthesized plant-based Zn NPs. The original peaks give maximum absorbance at 610 nm. It was observed that the degradation of dye increased with time under UV light. Fig 3.16 indicates the photocatalytic degradation of xylene dye for time intervals from 5 to 30 min. 60% removal of dye occurs in 30 minutes.

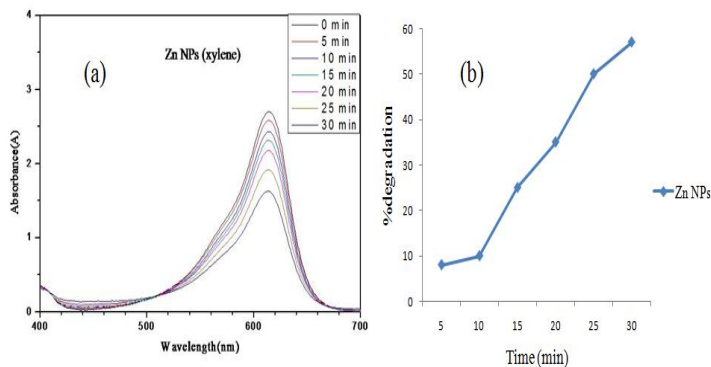


Figure 3.16: Degradation of xylene dye by ZnO NPs

Photocatalytic Degradation of Congo red dye by CuO NPs

The photocatalytic degradation of Congo red dye under the UV light by CuO NPs was studied to check the Degradation of Congo red dye and the maximum absorbance of the original peak was observed at 490 nm and the degradation increased over time from 5 to 30 mints. 90% removal of dye occurred at 30 minutes. Fig 3.17 illustrate the degradation of Congo red dye by CuO NPs.

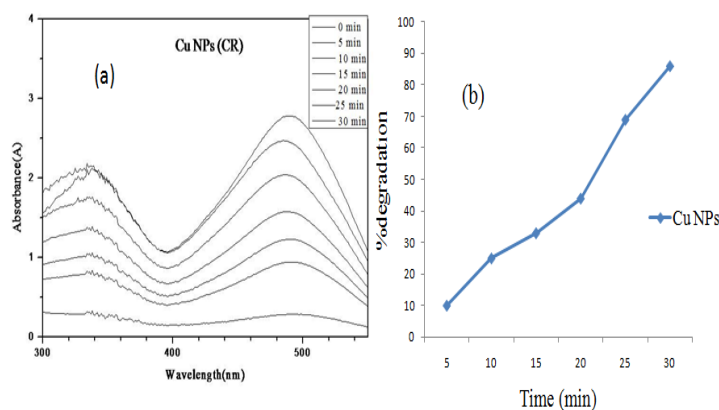


Figure 3.17: Degradation of Congo red dye by CuO NPs

DISCUSSION

Nanotechnology is relevant to diverse fields of science and technology. Due to the many advantages over non-biological systems, several research groups have exploited the use of biological systems for the synthesis of nanoparticles. Plants are efficient candidates for the fabrication of metal nanoparticles. In the present study zinc and copper nanoparticles were synthesized using *Caralluma tuberculata* stem extract. Different plants were reported by other similar studies like the peels extract of *Punica granatum* [14], *Hibiscus subdaria* leaf extract [15], Aloe vera leaf extract [16], and leaf extract of *Cyanometra ramiflora* [17], for the synthesis of zinc oxide nanoparticles. For the synthesis of copper nanoparticles *Ocimum basilicum* leaf extract [18], *Eichhornia crassipes* leaf extract [19], Aloe vera leaf extract [20], and leaf extract of *Ixoro coccinea* [21] were reported.

In the present study, the characterization of ZnO NPs and CuO NPs was done by different techniques i.e., color change, UV (UV–visible spectroscopy), Fourier Transform Infrared Spectroscopy (FT-IR), EDX, and Scanning Electron Microscopy (SEM). In previous studies, the formation of green synthesized ZnO NPs was confirmed by UV-VIS spectroscopic absorbance showing peaks at 364 nm [22], and 325 nm [23]. For copper nanoparticles, absorbance in the range of 460 nm has been used as an indicator to confirm the formation of CuO NPs as shown in Fig 3.2. In a previous study, the formation of green synthesized CuO NPs was confirmed by UV-VIS spectroscopic absorbance showing a peak at 275nm (Berra, D. et al., 2018), and 285 nm [24].

The FTIR Spectra of the extract showed a broad peak in the range of 3500-3000 cm^{-1} , which might be due to the -OH group. The spectra also showed peaks in the region of 1600 cm^{-1} , which might be due to the starching vibration of C=O and C=C stretch. The acetone extraction shows peaks in the range of 3100-2900 cm^{-1} , which is due to the stretching vibration of C-H. The acetone extraction sample also showed a peak at 1350-1250 cm^{-1} , which might be due to the C-O-C as shown in Fig 3.3. FT-IR spectrum of synthesized ZnO NPs also showed peaks at about 1600 cm^{-1} , 1000 cm^{-1} , and 800-550 cm^{-1} , as shown in Fig 3.4 which represents that ZnO NPs are successfully synthesized. FT-IR spectrum of synthesized CuO NPs showed broad peaks in the range of 3500-3000 cm^{-1} , 1700-1600 cm^{-1} , 1000 cm^{-1} , and below 900 cm^{-1} , as shown in Fig 3.5 which indicated that CuO NPs were successfully synthesized. In the

previous study, FT-IR spectrum of *Phoenix dactylifera* leaf extract depicted some peaks at 3264, 1605, 1442, 1283 and 1049 cm^{-1} . The broad band, at 3264 cm^{-1} , is due to the O–H group stretching vibration. The absorption peaks situated around 1605, 1442, 1283, 1049 cm^{-1} correspond to the stretching vibrations of C=C, C–C, C–H, and C–O. Comparing the spectrum of the synthesized CuO NPs with extract showed a weak peak at 512 and 618 cm^{-1} which are attributed to vibrations of CuO confirming the formation of CuO NPs [25]. By FT–IR analysis of *Rheum palmatum* L. root extract, peaks at 3400–3500, 1680, 1450, and 1050–1270 cm^{-1} are observed, which correspond to the free OH in the molecule and OH group forming hydrogen bonds, carbonyl group (C=O), stretching C=C aromatic ring, and C–OH stretching vibrations [26]. In the FTIR spectrum of green tea, the band at 3394 cm^{-1} is due to stretching vibrations of O–H groups and N–H stretching. The C–H stretch and O–H stretch appear at 2926 and 2864 cm^{-1} respectively. The strong band at 1627 cm^{-1} is attributed to the C=C and C=O stretch. The C–N gives the band at 1396 cm^{-1} . The C–O–C stretching gives a band at 1741 cm^{-1} and C–O stretching causes a band at 1037 cm^{-1} . The presence of a higher percentage of the phenolic group of molecules is responsible for the reduction process and the amino acids and amide linkages in protein are responsible for the stabilization of the ZnO NPs [23]. The ZnO NPs were compared to *T. pallida* aqueous leaf extract. The peak at 1450–1500 cm^{-1} corresponds to N–H stretching vibrations. ZnO NP stretching was identified at 400–800 cm^{-1} , O–H stretching at 3433 cm^{-1} , and aldehyde C–H stretching at 2934 cm^{-1} . A protein peak was observed at 1250 – 1270 cm^{-1} ; thus, the ZnO NPs were covered with a layer of primary and secondary metabolites [27].

In the present study, the SEM images revealed that the synthesized ZnO NPs were spherical. The size of the ZnO NPs was also calculated by using Image j software which was 40nm and the particles were dispersing as shown in Fig 3.6. SEM images of the synthesized CuO NPs showed that nanoparticles were irregular in shape with an average size of 60 nm and there was agglomeration between the nanoparticles as shown in Fig 3.7. In contrast to our study, SEM micrographs displayed that the green synthesized ZnO NPs were dispersed, and the average size ranged from 25 to 40 nm and spherical [28] while in another study ZnO NPs were observed with an average size of 50-100nm [29]. The morphology of the ZnO NPs was uneven where they comprised of heterogeneous particles with uniform spheres that had an average size of 29 nm, with elongated and rod-like structures measuring 70 nm [30]. CuO NPs had an average size ranging from 22-28 nm. SEM survey shows that the obtained nanoparticles have in general a spherical shape [31].

In the present study, EDX spectroscopy of ZnO NPs showed two strong peaks for the zinc atom at 1 keV and 8.5 keV, a single peak for the oxygen atom at 0.5 keV with a weight percentage of 34.69% zinc and 39.30% oxygen affirmed the successful synthesis and purity of ZnO NPs as shown in Fig 3.8, while EDX spectroscopy of CuO NPs showed two strong peaks of copper at 1 keV and 8 keV and a single peak for oxygen atom at 0.5 keV with the weight percentage of Copper 16.13% and oxygen 35.42% affirmed the successful synthesis and purity of CuO NPs as shown in Fig 3.9. In previous studies EDX of ZnO NPs showed peaks for zinc atoms at 1 keV and 9 keV and for oxygen atoms at 0.5 keV with a weight percentage of Zn 55.92% and oxygen 44.08% proves ZnO NPs [32]. The elements present in the ZnO NPs were analyzed using the EDX spectrum and showed two strong peaks for the zinc atom at 1 keV and 8.7 keV, respectively, and a single peak for the oxygen atom at 0.5 keV, which are the characteristic features of ZnO NPs [33]. EDX spectra of CuO NPs showed peaks for copper at 1 keV and 8 keV and for oxygen at 0.5 keV with a weight percentage of 36.955% Cu and 52.09% oxygen [34]. In the current study, the synthesized ZnO NPs and CuO NPs showed remarkable antibacterial activity against two bacterial strains staphylococcus aureus and Acetobacter. ZnO NPs were equally effective against both strains as shown in Fig 3.10. The antibacterial activity of CuO NPs against *Staphylococcus aureus* was higher as compared to *Acetobacter* as shown in Fig 3.12 while a hybrid of ZnO and CuO NPs showed significant activity against both tested bacterium as shown in Fig 3.14. The higher

antibacterial activity was certainly due to zinc and copper cations released from ZnO NPs and CuO NPs as negatively charged bacterial cell wall is more attracted to zinc and copper ions causing bacterial cell wall rupture and finally cell death. Previous studies reported excellent bactericidal activity shown by ZnO NPs on Gram-positive *Bacillus licheniformis* and *Bacillus pumilis* and Gram-negative *Escherichia coli* and *Proteus vulgaris* bacteria [35]. The antibacterial activities of ZnO NPs against pathogenic strains Gram-negative bacterial species, *Klebsiella pneumoniae*, *Pseudomonas aeruginosa*, and *Escherichia coli*, and the Gram-positive *Staphylococcus aureus* were studied which indicated better antibacterial activity of the ZnO NPs [36]. In a previous study, CuO NPs showed excellent antibacterial activity for pathogens like *Staphylococcus pneumonia*, *Streptococcus aureus*, and *Klebsiella pneumonia* [37]. *Escherichia coli* and *Staphylococcus aureus* by the observation of inhibition zones around each well [18].

In the current study, the synthesized ZnO NPs and CuO NPs showed remarkable photocatalytic dye degradation activity. The photocatalytic degradation of xylene dye under UV light was studied to check the removal of dye by measuring the decrease in absorbance of dye in the presence of the synthesized ZnO NPs. The photocatalytic degradation of Congo red dye under UV light by CuO NPs was studied to check the degradation of CR dye. Previous studies reported the photocatalytic activity of ZnO NPs to degrade cationic and anionic dyes, including malachite green (MG), Congo red (CR), methylene blue (MB), and eosin Y (EY), under ultraviolet illumination were studied. The photocatalyst degraded approximately 99% of the MG, MB, CR, and EY dyes within 70, 70, 80, and 90 min of contact time, respectively, at a dye concentration of 15 mg/L, 5 mg/L, ZnO NPs degraded 100% of the MG, MB, CR, and EY dyes within 23, 25, 28, and 30 min, respectively [38]. Mg of ZnO NPs removed 100% of the methylene blue solution (32 mg/L) within 60 min and 100 mg was required for the complete removal of rhodamine B (9.5 mg/L) within 50 min [30]. Previous studies reported the photocatalytic activity of CuO NPs using crystal violet for dye degradation activity. The efficiency of CuO NPs for the Degradation of CV at 585–590 nm at different time intervals was assessed. Initially, after 60 min of incubation, a strong indication of Cu^+ ion generation was detected by the change of light blue color of the solution but after 120 min of incubation, a complete disappearance of color in the reaction mixture was observed. In the presence of CuO NPs, the primary absorption peak at 586 nm decreased slowly with the increasing sunlight exposure time. This indicated the photocatalytic Degradation of CV dye in the presence of CuO NPs [39]. The nature of the synthesized CuO NPs as photo-catalyst was evident from the disintegration phenomenon in which the organic nature commercial grade Acid Black 210 dye was degraded by the nanoparticles. The CuO NPs completely disintegrated the Acid Black 210 dye into CO_2 and H_2O within one hour [34].

CONCLUSION

From the present study, it was concluded that the synthesis of nanoparticles by the biological method is a good alternative as compared to hazardous physical and chemical methods. The UV- Vis Spectrophotometer showed the indication for the formation of zinc oxide and copper oxide nanoparticles. Study confirmed the shift of metallic ions into nanoparticles and SEM revealed the morphological properties. The elemental presence of zinc and copper was confirmed with EDX analysis. Results indicated the effectiveness of nanoparticles against different bacterial strains. In the current study, the synthesized zinc oxide and copper oxide nanoparticles showed remarkable antibacterial activity against *staphylococcus aureus* and *Acetobacter*. ZnO nanoparticles illustrated the catalytic degradation of xylene dye and CuO nanoparticles illustrated the catalytic degradation of Congo red dye and showed very positive degradation results. Our research work showed that NPs play an important role in biological assays and photocatalytic degradation.

References

1. **Behera, A. L., Patil, S. V., Sahoo, S. K., & Sahoo, S. K. (2010).** Nanosizing of drugs: A promising approach for drug delivery. *Der Pharmacia Sinica*, 1(1), 20-28.
2. **Roco, M. C. (2003).** Nanotechnology: convergence with modern biology and medicine. *Current opinion in biotechnology*, 14(3), 337-346.
3. **Vélez, M. A., Perotti, M. C., Santiago, L., Gennaro, A. M., & Hynes, E. (2017).** Bioactive compounds delivery using nanotechnology: design and applications in dairy food. In *Nutrient delivery* (pp. 221-250). Academic Press.
4. **Bera, A., & Belhaj, H. (2016).** Application of nanotechnology by means of nanoparticles and nanodispersions in oil recovery-A comprehensive review. *Journal of Natural Gas Science and Engineering*, 34, 1284-1309.
5. **Fernandes, C., Benfeito, S., Fonseca, A., Oliveira, C., Garrido, J., Garrido, E. M., & Borges, F. (2017).** Photodamage and photoprotection: toward safety and sustainability through nanotechnology solutions. In *Food preservation* (pp. 527-565). Academic Press.
6. **Frewer, L. J., Gupta, N., George, S., Fischer, A. R. H., Giles, E. L., & Coles, D. (2014).** Consumer attitudes towards nanotechnologies applied to food production. *Trends in food science & technology*, 40(2), 211-225.
7. **Hussein, A. K. (2016).** Applications of nanotechnology to improve the performance of solar collectors—Recent advances and overview. *Renewable and Sustainable Energy Reviews*, 62, 767-792.
8. **Sharif, M. K., Butt, M. S., & Sharif, H. R. (2017).** Role of nanotechnology in enhancing bioavailability and delivery of dietary factors. In *Nutrient delivery* (pp. 587-618). Academic Press.
9. **Syedmoradi, L., Daneshpour, M., Alvandipour, M., Gomez, F. A., Hajghassem, H., & Omidfar, K. (2017).** Point of care testing: The impact of nanotechnology. *Biosensors and Bioelectronics*, 87, 373-387.
10. **Kreibig, U., & Vollmer, M. (1995).** Quasistatic response of a small metal sphere to an electric field. *Optical properties of metal clusters*, 25,483-525.
11. **Mallick, K., Witcomb, M. J., & Scurrall, M. S. (2006).** Palladium Nanoparticles in Poly (o-phenylenediamine): Synthesis of a Nanostructured 'Metal-Polymer' Composite Material. *Journal of Macromolecular Science Part A: Pure and Applied Chemistry*, 43(9), 1469-1476.
12. **Schultz, S., Smith, D. R., Mock, J. J., & Schultz, D. A. (2000).** Single-target molecule detection with nonbleaching multicolor optical immunolabels. *Proceedings of the National Academy of Sciences*, 97(3), 996-1001.
13. **Kalaiarasi, R., Jayallakshmi, N., & Venkatachalam, P. (2010).** Plant Cell Biotechnol. *Mol. Biol*, 11(1).
14. **Mishra, V., & Sharma, R. (2015).** Green synthesis of zinc oxide nanoparticles using fresh peels extract of Punica granatum and its antimicrobial activities. *International Journal of Pharma Research and Health Sciences*, 3(3), 694-699.
15. **Bala, N., Saha, S., Chakraborty, M., Maiti, M., Das, S., Basu, R., & Nandy, P. (2015).** Green synthesis of zinc oxide nanoparticles using Hibiscus subdariffa leaf extract: effect of temperature on synthesis, antibacterial activity and anti-diabetic activity. *RSC Advances*, 5(7), 4993-5003.
16. **Senthilkumar, S. R., & Sivakumar, T. (2014).** Green tea (Camellia sinensis) mediated synthesis of zinc oxide (ZnO) nanoparticles and studies on their antimicrobial activities. *Int J Pharm Pharm Sci*, 6(6), 461-465.
17. **Varadavenkatesan, T., Lyubchik, E., Pai, S., Pugazhendhi, A., Vinayagam, R., & Selvaraj, R. (2019).** Photocatalytic Degradation of Rhodamine B by zinc oxide nanoparticles synthesized using the leaf extract of Cyanometra ramiflora. *Journal of Photochemistry and Photobiology B: Biology*, 199, 111621.

18. **Altikatoglu, M., Attar, A., Erci, F., Cristache, C. M., & Isildak, I. (2017).** Green synthesis of copper oxide nanoparticles using *Ocimum basilicum* extract and their antibacterial activity. *Fresenius Environ Bull*, 25(12), 7832-7837.
19. **Sultan, K., Zakir, M., Khan, H., Khan, I. U., Rehman, A., Akber, N. U., & Khan, M. A. (2014).** The effect of extract/fractions of *Caralluma tuberculata* on blood glucose levels and body weight in alloxan-induced diabetic rabbits. *Journal of evidence-based complementary & alternative medicine*, 19(3), 195-199.
20. **Kumar, P. V., Shameem, U., Kollu, P., Kalyani, R. L., & Pammi, S. V. N. (2015).** Green synthesis of copper oxide nanoparticles using *Aloe vera* leaf extract and its antibacterial activity against fish bacterial pathogens. *BioNanoScience*, 5(3), 135-139.
21. **Vishveshvar, K., Krishnan, M. A., Haribabu, K., & Vishnuprasad, S. (2018).** Green synthesis of copper oxide nanoparticles using *Ixiro coccinea* plant leaves and its characterization. *BioNanoScience*, 8(2), 554-558.
22. **Mishra, V., & Sharma, R. (2015).** Green synthesis of zinc oxide nanoparticles using fresh peels extract of *Punica granatum* and its antimicrobial activities. *International Journal of Pharma Research and Health Sciences*, 3(3), 694-699.
23. **Senthilkumar, S. R., & Sivakumar, T. (2014).** Green tea (*Camellia sinensis*) mediated synthesis of zinc oxide (ZnO) nanoparticles and studies on their antimicrobial activities. *Int J Pharm Pharm Sci*, 6(6), 461-465.
24. **Yugandhar, P., Vasavi, T., Devi, P. U. M., & Savithramma, N. (2017).** Bioinspired green synthesis of copper oxide nanoparticles from *Syzygium alternifolium* (Wt.) Walp: characterization and evaluation of its synergistic antimicrobial and anticancer activity. *Applied Nanoscience*, 7(7), 417-427.
25. **Berra, D., Laouini, S. E., Benhaoua, B., Ouahrani, M. R., Berrani, D., & Rahal, A. (2018).** Green synthesis of copper oxide nanoparticles by *Pheonix dactylifera* L leaves extract. *Digest Journal of Nanomaterials and Biostructures*, 13, 1231-1238.
26. **Bordbar, M., Sharifi-Zarchi, Z., & Khodadadi, B. (2017).** Green synthesis of copper oxide nanoparticles/clinoptilolite using *Rheum palmatum* L. root extract: high catalytic activity for reduction of 4-nitro phenol, rhodamine B, and methylene blue. *Journal of Sol-Gel Science and Technology*, 81(3), 724-733
27. **Li, C. Y., Zhang, Z. C., Mao, J. Y., Shi, L. F., Zheng, Y., & Quan, J. L. (2017).** Preparation of *Tradescantia pallida*-mediated zinc oxide nanoparticles and their activity against cervical cancer cell lines. *Tropical Journal of Pharmaceutical Research*, 16(3), 494-500.
28. **Sangeetha, G., Rajeshwari, S., & Venckatesh, R. (2011).** Green synthesis of zinc oxide nanoparticles by *aloe barbadensis miller* leaf extract: Structure and optical properties. *Materials Research Bulletin*, 46(12), 2560-2566.
29. **Mishra, V., & Sharma, R. (2015).** Green synthesis of zinc oxide nanoparticles using fresh peels extract of *Punica granatum* and its antimicrobial activities. *International Journal of Pharma Research and Health Sciences*, 3(3), 694-699.
30. **Prasad, A. R., Garvasis, J., Oruvil, S. K., & Joseph, A. (2019).** Bio-inspired green synthesis of zinc oxide nanoparticles using *Abelmoschus esculentus* mucilage and selective degradation of cationic dye pollutants. *Journal of Physics and Chemistry of Solids*, 127, 265-274.
31. **Rajeshkumar, S., Menon, S., Kumar, S. V., Tambuwala, M. M., Bakshi, H. A., Mehta, M., & Dua, K. (2019).** Antibacterial and antioxidant potential of biosynthesized copper nanoparticles mediated through *Cissus arnotiana* plant extract. *Journal of Photochemistry and Photobiology B: Biology*, 197, 111531.
32. **Gnanasangeetha, D., & SaralaThambavani, D. (2013).** One pot synthesis of zinc oxide nanoparticles via chemical and green method. *Res J Mater Sci*, 2320, 6055.

33. **Varadavenkatesan, T., Lyubchik, E., Pai, S., Pugazhendhi, A., Vinayagam, R., & Selvaraj, R. (2019).** Photocatalytic Degradation of Rhodamine B by zinc oxide nanoparticles synthesized using the leaf extract of *Cyanometra ramiflora*. *Journal of Photochemistry and Photobiology B: Biology*, 199, 111621.
34. **Ijaz, F., Shahid, S., Khan, S. A., Ahmad, W., & Zaman, S. (2017).** Green synthesis of copper oxide nanoparticles using *Abutilon indicum* leaf extract: Antimicrobial, antioxidant and photocatalytic dye degradation activities. *Tropical Journal of Pharmaceutical Research*, 16(4), 743-753.
35. **Ishwarya, R., Vaseeharan, B., Kalyani, S., Banumathi, B., Govindarajan, M., Alharbi, N. S., & Benelli, G. (2018).** Facile green synthesis of zinc oxide nanoparticles using *Ulva lactuca* seaweed extract and evaluation of their photocatalytic, antibiofilm and insecticidal activity. *Journal of Photochemistry and Photobiology B: Biology*, 178, 249-258.
36. **Senthilkumar, S. R., & Sivakumar, T. (2014).** Green tea (*Camellia sinensis*) mediated synthesis of zinc oxide (ZnO) nanoparticles and studies on their antimicrobial activities. *Int J Pharm Pharm Sci*, 6(6), 461-465.
37. **Hemalatha, S., & Makeswari, M. (2017).** Green synthesis, characterization and antibacterial studies of CuO nanoparticles from *Eichhornia crassipes*. *Rasayan J. Chem*, 10(3), 838-843.
38. **Rupa, E. J., Kaliraj, L., Abid, S., Yang, D. C., & Jung, S. K. (2019).** Synthesis of a zinc oxide nanoflower photocatalyst from sea buckthorn fruit for degradation of industrial dyes in wastewater treatment. *Nanomaterials*, 9(12), 1692.
39. **Vasantharaj, S., Sathiyavimal, S., Saravanan, M., Senthilkumar, P., Gnanasekaran, K., Shanmugavel, M., & Pugazhendhi, A. (2019).** Synthesis of ecofriendly copper oxide nanoparticles for fabrication over textile fabrics: characterization of antibacterial activity and dye degradation potential. *Journal of Photochemistry and Photobiology B: Biology*, 191, 143-149.